Inorganic Chemistry

Article

pubs.acs.org/IC

Role of Aggregation in the Synthesis and Polymerization Activity of SalBinap Indium Alkoxide Complexes

Dinesh C. Aluthge, Ellen X. Yan, Jun Myun Ahn, and Parisa Mehrkhodavandi*

Department of Chemistry, University of British Columbia, 2036 Main Mall, Vancouver, British Columbia, Canada

Supporting Information

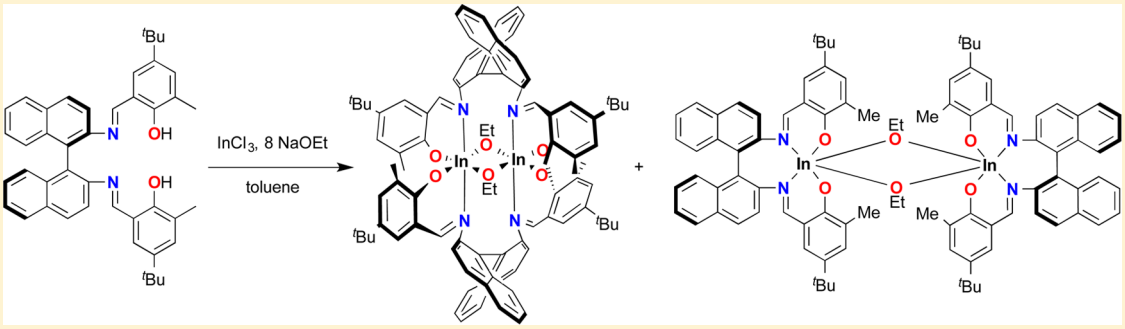

ABSTRACT: The reaction of racemic SalBinap ligand, (±)-H_2(**ONN*O$_{Me}$**), with $InCl_3$ and excess NaOEt generated a mixture of two dinuclear compounds [(μ–κ^2-ONN*O$_{Me}$)In(μ-OEt)]$_2$ (**1a**) and [κ^4-ONN*O$_{Me}$)In(μ-OEt)]$_2$ (**1b**), which were isolated and fully characterized. Polymerization of racemic lactide with **1a** and **1b** was slow in refluxing THF and showed only modest stereoselectivity. Catalyst **1b** displayed better control than **1a**, with the experimental molecular weights of the resulting poly(lactic acid) in agreement with the expected values. The higher-than-expected molecular weights observed in polymers formed by **1a** were due to partial initiation of the catalyst. The reaction of (±)-H_2(**ONN*O$_{tBu}$**) with $InCl_3$ yielded (κ^4-ONN*O$_{tBu}$)InCl (**2**); however, further reactivity of the compound formed a mixture of products. An attempt to prevent aggregation by reacting (±)-H_2(**ONN*O$_{Me}$**) with $InCl_3$ and excess NaO^{i}Pr yielded an intractable mixture, including [(μ–κ^2-ONN*O$_{Me}$)In]$_2$(μ-Cl)(μ-OH) (**3**). The thermal stabilities of compounds **1a** and **1b** under polymerization conditions were investigated. Examination of the polymerization behavior of complexes **1a** and **1b** and the reaction equilibrium between the two illustrates the importance of aggregation in indium salen complexes compared to their aluminum counterparts.

INTRODUCTION

The development of chiral metal-based catalysts for the stereoselective polymerization of racemic lactide (*rac*-LA) to generate isotactic and stereoblock poly(lactic acid) (PLA) has attracted considerable interest over the past 20 years.[1] Spassky et al. introduced an aluminum methoxide complex supported by a chiral SalBinap ligand as an effective catalyst for the stereoselective polymerization of racemic lactide (Chart 1A).[2] Development of bulkier initiators and mechanistic studies of the system established the highly isoselective nature of this class of compounds and provided evidence for generation of stereoblock PLA.[3] This work was extended to chiral aluminum complexes bearing the Jacobsen ligand (Chart 1B)[4] as well as a number of analogous achiral aluminum complexes capable of some degree of selective polymerization of *rac*-LA.[5] Thus, aluminum alkoxide initiators supported by tetradentate Schiff-base (salen) ligands remain the standard for site-selective and highly isoselective catalysts capable of forming stereoblock PLA.[1] The chiral salen motif has been used successfully by a number of groups to generate selective catalysts with aluminum and other trivalent metals as well as with functionalized salen derivatives.[6] One characteristic of some salen aluminum alkoxide initiators is their tendency to aggregate and form multiple complexes.[7] In particular, unsubstituted SalBinap ligands can bridge two metal centers in a κ^2 binding mode (Chart 1C).[8]

We are interested in the ring-opening polymerization (ROP) of cyclic esters by indium amino phenolate complexes.[9] In particular, we have been exploring the importance of aggregation in indium catalysts and the involvement of two metal centers in indium-catalyzed polymerization reactions.[10] Other groups have also explored indium catalyzed polymerization reactions[11] and investigated the differences in reactivity between aluminum salen complexes and the indium analogues with the larger ionic radius.[6g,12] The chemistry of indium salen alkoxide complexes has been explored by Atwood et al., and different modes of aggregation in these compounds, including dimer formation (Chart 1E), have been reported.[13]

Recently, we reported that an indium-ethoxide initiator supported by the Jacobsen salen ligand is a highly active and isoselective catalyst for lactide polymerization (Chart 1D).[14] Herein we expand our studies to SalBinap-indium alkoxide catalysts and report on their reactivity for the polymerization of

Received: March 21, 2014
Published: June 10, 2014

   dx.doi.org/10.1021/ic500647j | *Inorg. Chem.* 2014, 53, 6828–6836

Chart 1. Al and In Salen Complexes[2,3d,4a,8,13a,b,14]

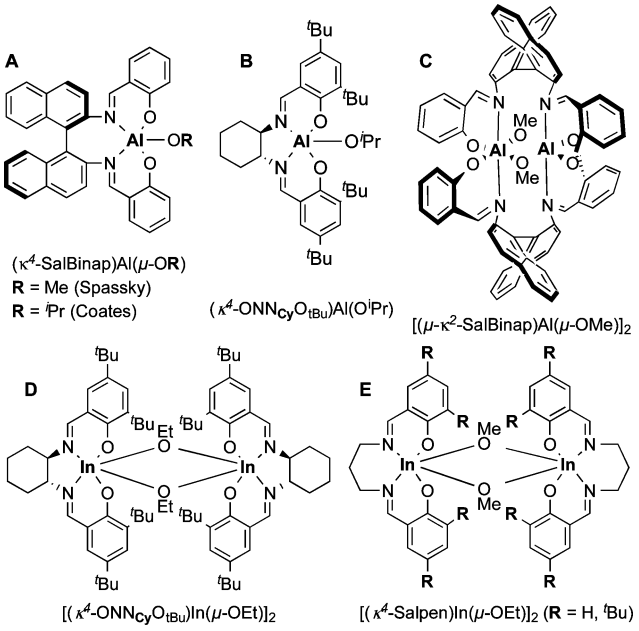

rac-LA. We also compare their reactivity to the aluminum analogues and show that structure−function relationships in dinuclear indium based compounds are not the same as in the aluminum analogues due to the larger ionic radii of the metal centers in In(III) complexes.

RESULTS AND DISCUSSION

Synthesis of Indium Complexes. The proligand *rac*-2,2′-[1,1′-binaphthalene-2,2′-diyl-bis(nitrilomethylidyne)]-bis-4-*tert*-butyl-6-methylphenol, (±)-H_2(**ONN*O$_{Me}$**), can be prepared in 94% yield by condensing *rac*-1,1′-binaphthyl-2,2′-diamine with 2 equiv of 4-*tert*-butyl-6-methylsalicylaldehyde. The ^{1}H NMR spectrum of (±)-H_2(**ONN*O$_{Me}$**) contains one singlet for the equivalent N=C*H* protons at 8.60 ppm. The use of the unsubstituted SalBinap proligand results in intractable and insoluble metal complex aggregates; these will not be discussed further.

Indium complexes are generated by the one-pot reaction of (±)-H_2(**ONN*O$_{Me}$**) (∼80 mM) with $InCl_3$ and excess NaOEt at room temperature in toluene. Analysis of the mixture with ^{1}H NMR spectroscopy after 16 h shows the formation of two products: **1a** and **1b** (Scheme 1). Stirring this mixture at room temperature for an additional 4 days forms the dinuclear complex [(μ−κ^2-ONN*O$_{Me}$)In(μ-OEt)]$_2$ (**1a**) as the sole product in 67% isolated yield (see below for **1b**). The optimum reaction time for synthesis of **1a** is dependent on the reaction concentration; more dilute reactions take longer to reach completion.

The ^{1}H NMR spectrum of **1a** contains two singlets at 8.61 and 8.58 ppm corresponding to the N=C*H* protons. Due to the highly symmetric nature of the complex only one resonance is observed for the aryl −CH_3 and −C(CH_3)$_3$ protons at 2.37 and 1.00 ppm, respectively. The signals for the OCH_2CH$_3$ methylene protons appear as two diastereotopic resonances at ∼2.10 and ∼2.80 ppm, and the OCH$_2$CH_3 resonances appear as a triplet at −0.44 ppm. Notably, the ethoxide shifts are considerably more upfield than those reported for other indium ethoxide complexes; for [(κ^4-ONN$_{Cy}$O$_{tBu}$)In(μ-OEt)]$_2$ (**D**) the −OCH_2CH$_3$ protons resonate at 3.61−3.40 ppm and the −OCH$_2$CH_3 protons resonate at 1.07 ppm. This upfield shift can be attributed to an induced magnetic field due to the aromatic ring current of the naphthyl moieties directly above each ethoxide.[15] Excess sodium is not observable in the product.

Single crystals of **1a** were obtained from a solution of the complex in hot acetonitrile, and its molecular structure was determined using single crystal X-ray crystallography. Complex **1a** is a dimer with two indium centers bridged by the OEt ligand as well as (**ONN*O$_{Me}$**) in κ^2 coordination mode (Figure 1). The D_2 symmetric complex contains two slightly distorted octahedral indium metal centers that are coplanar with the bridging oxygen atoms of the ethoxide groups. The homochiral dimer crystallized in the centrosymmetric $P\bar{1}$ space group, indicating the presence of both the *S,S*- and *R,R*-dimers in the unit cell. The highly symmetric solution structure confirms that **1a** is also homochiral in solution.

Complex **1b** can be isolated from a 1:1 mixture of **1a** and **1b** generated in a reaction carried out at room temperature for 16 h. Complex **1a** is then extracted with acetonitrile from this mixture leaving [(κ^4-ONN*O$_{Me}$)In(μ-OEt)]$_2$ (**1b**) as the insoluble component. The ^{1}H NMR spectrum of **1b** in $CDCl_3$ contains two well-separated signals at 8.33 and 7.93 ppm corresponding to the N=C*H* protons. The loss of symmetry in **1b**, compared to **1a**, is clear from the presence of two sets of resonances for the aryl −CH_3 (2.01 and 1.87 ppm) and −C(CH_3)$_3$ (1.35 and 1.23 ppm) protons.

Scheme 1. Synthesis of [(μ-κ^2-ONN*O$_{Me}$)In(μ-OEt)]$_2$ (1a) and [(κ^4- ONN*O$_{Me}$)In(μ-OEt)]$_2$ (1b)

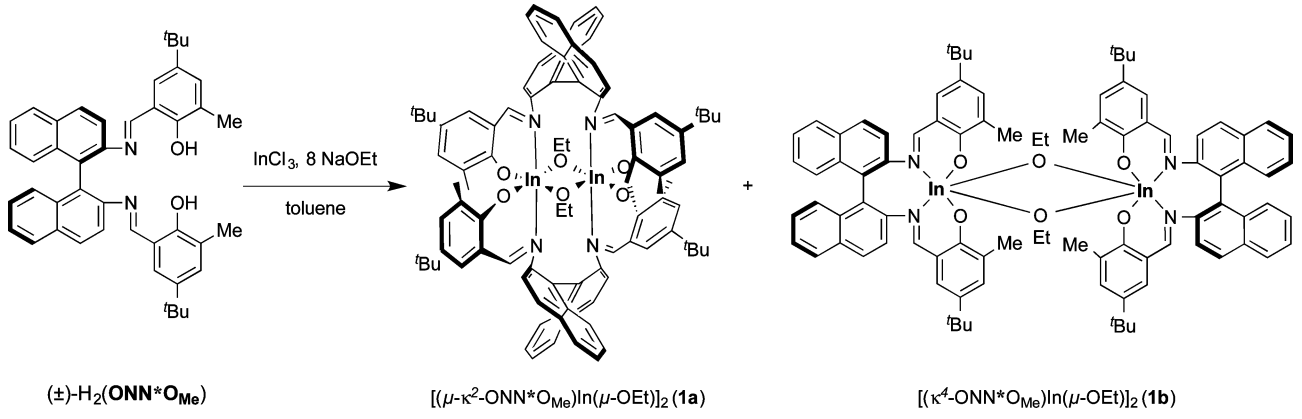

dx.doi.org/10.1021/ic500647j | Inorg. Chem. 2014, 53, 6828−6836

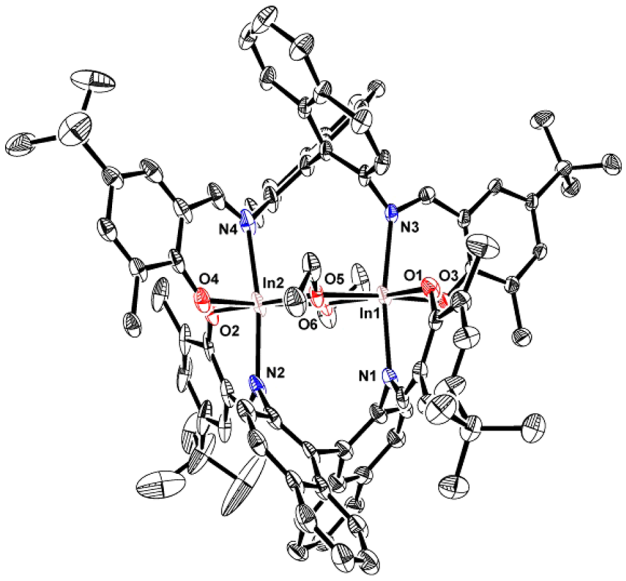

Figure 1. Molecular structure of **1a** depicted with ellipsoids at 50% probability (H atoms and solvent molecules omitted for clarity).

Single crystals of **1b** are obtained after slow evaporation in diethyl ether. The molecular structure of **1b** shows two distorted octahedral metal centers with κ^4 coordination of the (**ONN*O$_{Me}$**) ligand to one indium center (Figure 2). The two

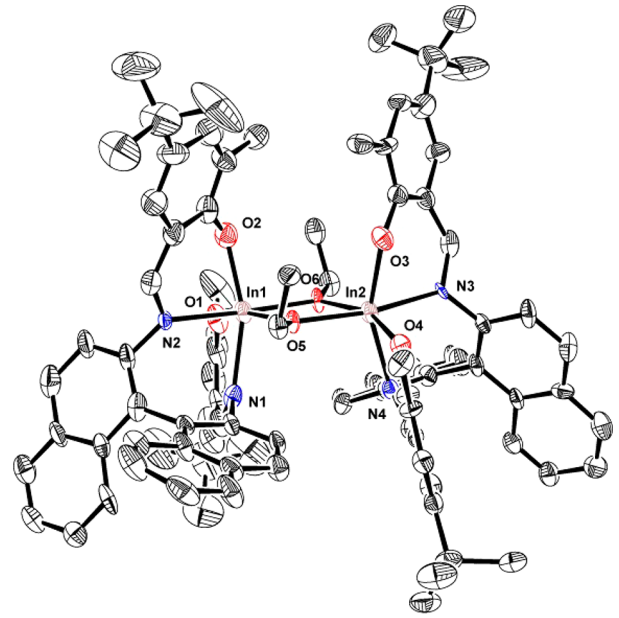

Figure 2. Molecular structure of **1b** depicted with ellipsoids at 50% probability (H atoms and solvent molecules omitted for clarity).

metal centers are bridged by ethoxide ligands. Notably, the In−N bond distances in **1b** (2.257(9)−2.318(6) Å) are longer than the corresponding bonds in [(κ^4-ONN$_{Cy}$O$_{tBu}$)In(μ-OEt)]$_2$ (**D**)[14] (2.206(6)−2.259(6) Å) and [(κ^4-Salpen)In(OMe)])$_2$ (**E**)[13a] (2.222(8)−2.263(7) Å), both of which contain the more electron rich CH$_2$−N$_{imine}$ moiety.

The structural motifs we observe for **1a** and **1b** have been previously reported for aluminum[7] and indium[13a] salen complexes, although a dimeric motif such as **1b** is most common with indium complexes. Complex **1a** is structurally similar to the dinuclear aluminum SalBinap complex [(μ−κ^2-SalBinap)Al(μ-OMe)]$_2$ (**C**) (Chart 1).[8] The In−(μ-O) bond distances are longer than the corresponding Al−(μ-O) bond distances (2.142(3)−2.165(3) Å vs 1.892(4)−1.895(4) Å). Bond angles around the octahedral cores of the Al and In compounds are similar (Supporting Information Figure S19). Similar κ^2 bound 6-coordinate salen indium alkoxide complexes were first reported by Atwood et al.[13a] While 6-coordinate dimeric [(κ^4-salen)Al(OR)]$_2$ complexes are known,[7] the most common coordination number for salen Al alkoxide complexes is five.[13c] In contrast, the larger ionic radius of In(III) often favors 6-coordinate complexes.[16] In particular, alkoxide complexes are prone to aggregation and can form dimeric [(κ^4-ligand)In(OR)]$_2$ complexes such as **D** or **E** or with dithiaalkanediyl-bridged bis(phenolato) (OSSO) complexes of indium.[17]

The solution structures of **1a** and **1b**, determined using pulsed gradient spin−echo (PGSE) spectroscopy, show that they are dinuclear in solution as well as in the solid state (Supporting Information Figure S17).[18] The diffusion coefficient of the proligand H$_2$(ONN*O), determined using PGSE at 25 °C with tetrakis(trimethylsilyl)silane (TMSS) as an internal standard, is 8.9(4) × 10^{-10} m^2 s^{-1}. In contrast, **1a** and **1b** had significantly lower diffusion coefficients of 6.2(2) × 10^{-10} m^2 s^{-1} and 6.1(2) × 10^{-10} m^2 s^{-1}. This decrease (~25%) in the diffusion coefficient from the proligand to **1a** and **1b** supports a dinuclear solution state structure for these complexes.[10a,14,19] Variable temperature ^{1}H NMR spectroscopy for **1a** and **1b** (toluene-d_8, 25 °C − 80 °C) shows no change in the resonances for either complex, indicating that these dimers stay intact at elevated temperature (Supporting Information Figures S15 and S16).

Complex **1a** is the thermodynamic product generated from the reaction mixture of **1a** and **1b**; at elevated temperatures (80 °C in toluene) formation of **1a** reaches completion in ~72 h. However, this occurs within a mixture containing *an excess of NaOEt*. In contrast, heating a pure sample of **1b** at 100 °C in toluene-d_8 generates <5% of **1a** in 96 h (Supporting Information Figure S10). When an isolated sample of **1b** is stirred in toluene with 5 equiv of NaOEt for 16 h, the ^{1}H NMR spectrum of the reaction shows a **1a**:**1b** ratio of 1:2.75 confirming the accelerated conversion of **1b** to **1a** in the presence of NaOEt (Supporting Information Figure S13).

We also investigated a two-step route to the desired alkoxide complexes in an attempt to avoid a mixture of compounds. The process, as described previously for the synthesis of [(κ^4-ONN$_{Cy}$O$_{tBu}$)In(μ-OEt)]$_2$ (**D**),[14] involves the deprotonation of the proligand followed by salt metathesis with InCl$_3$. However, the deprotonation of (±)-H$_2$(**ONN*O$_{Me}$**) with 2 equiv of KO^{t}Bu and the subsequent salt metathesis with InCl$_3$ produces a mixture of two major species (Supporting Information Figure S7). We were not able to isolate these species for complete characterization; however, the ^{1}H NMR signals of the two compounds suggest that they may be chloro-bridged analogues of **1a** and **1b**. Treating this mixture with excess NaOEt yields a mixture of **1a** and **1b** (**1a**:**1b** ~1:2.5) (Supporting Information Figure S8).

In another attempt to control or prevent aggregation in our complexes using increased steric hindrance, we synthesized the known proligand (±)-H$_2$(**ONN*O$_{tBu}$**) in a similar manner to H$_2$(**ONN*O$_{Me}$**) (Scheme 2).[20] Deprotonation of (±)-H$_2$(**ONN*O$_{tBu}$**) with 2 equiv of KO^{t}Bu and subsequent salt metathesis with 1 equiv of InCl$_3$ forms (κ^4-ONN*O$_{tBu}$)-

dx.doi.org/10.1021/ic500647j | Inorg. Chem. 2014, 53, 6828−6836

Scheme 2. Formation of Complex 2

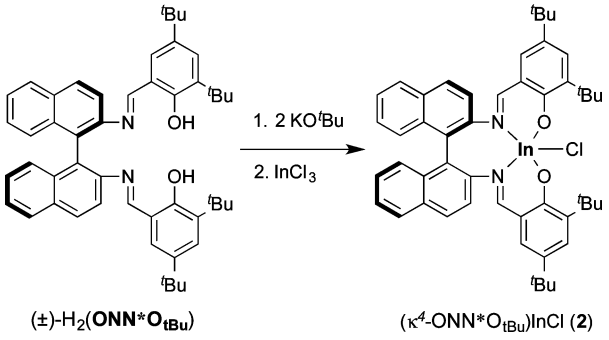

InCl (**2**) exclusively with an isolated yield of 59%. The ^{1}H NMR spectrum of **2** in $CDCl_3$ shows a broad singlet at 8.48 ppm corresponding to the N=C*H* resonances. This is in contrast to (κ^4-ONN$_{Cy}$O$_{tBu}$)InCl which shows two distinct ^{1}H NMR resonances for the imine protons.

Single crystals of **2** can be isolated from hexanes at ambient temperature using slow evaporation. The molecular structure of **2** shows a mononuclear indium complex with distorted trigonal bipyramidal geometry (Figure 3). The In−N bond distances are

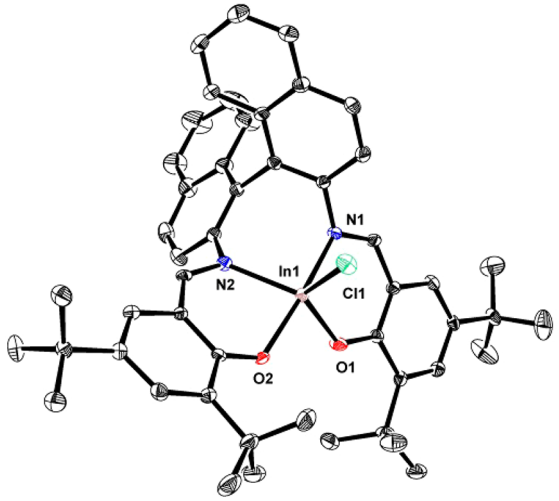

Figure 3. Molecular structure of **2** depicted with ellipsoids at 50% probability (H atoms and solvent molecules omitted for clarity).

slightly longer than those of (κ^4-ONN$_{Cy}$O$_{tBu}$)InCl (2.191(4)−2.219(3) vs 2.171(7)− 2.207(7) Å), while the In−O bond distances for the two complexes are similar (2.045(3)−2.065(3) for **2** vs 2.044(6)−2.050(6) Å).

Unfortunately, reactions of **2** with NaOEt under a variety of conditions produce an intractable mixture of products. One pot reactions of (±)-H$_2$(**ONN*O$_{tBu}$**) with NaOEt and $InCl_3$ under a variety of conditions also do not yield isolable complexes. Use of a bulkier alkoxide is a strategy utilized by Coates et al. to prevent the formation of aluminum complexes analogous to **1a**.[8] However, our attempts to replace NaOEt with NaO^{i}Pr resulted in intractable mixtures of products. Single crystals isolated from one such reaction after exposure to moisture shows the formation of [(μ−κ^2-ONN*O$_{Me}$)In]$_2$(μ-Cl)(μ-OH) (**3**) as one of many products (Figure 4). The molecular structure of **3** shows two octahedral indium centers bridged by two κ^2-(**ONN*O$_{Me}$**) as well as a bridging hydroxide and a

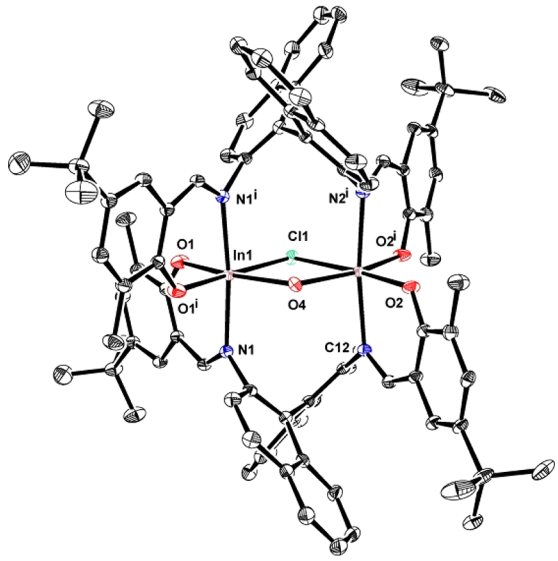

Figure 4. Molecular structure of **3** depicted with ellipsoids at 50% probability (H atoms and solvent molecules omitted for clarity).

bridging chloride. Attempts to use KOCH$_2$Ph instead of NaOEt also resulted in complex mixtures of products.

Our struggles in the synthesis of isolable dinuclear complexes are a testament to the difficulty of controlling aggregation phenomenon in indium alkoxide complexes. We have reported that hydroxyl-bridged complexes are readily generated from the hydrolysis of indium alkoxide groups with trace amounts of water.[9d,10a] Thus, it is possible that [(μ−κ^2-ONN*O$_{Me}$)In]$_2$(μ-Cl)(μ-O^{i}Pr) is one of the metal complexes generated in this reaction and complex **3** forms by the reaction of this species with adventitious water (Scheme 3). However, we have never

Scheme 3. Possible Route for Formation of 3

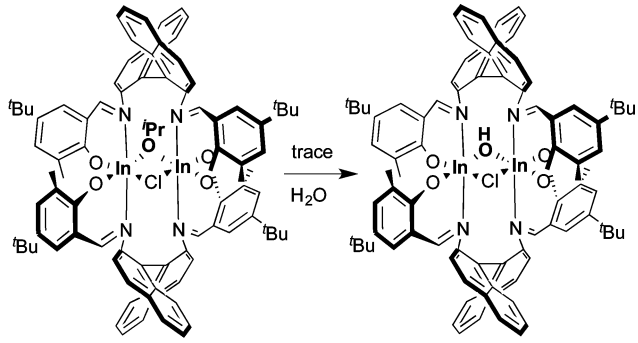

successfully isolated a pure sample of an indium isopropoxide complex with our proligands. It appears that a delicate balance of steric bulk is required to form stable indium dinuclear complexes, which are the thermodynamic products in these systems. This is further supported by the fact that, as discussed above, unsubstituted SalBinap ligands do not form isolable indium complexes like their aluminum analogues. Thus, although increasing the steric bulk of the complexes does prevent dimer formation, it also prevents formation of stable dinuclear complexes. Attempts to deviate from the thermodynamically stable dinuclear complexes only complicate the synthetic outcome of these reactions.

dx.doi.org/10.1021/ic500647j | Inorg. Chem. 2014, 53, 6828−6836

Table 1. Polymerization of *rac*-LA with In and Al Catalysts[a]

	catalyst	time (h)	conv (%)	$M_{n\,theo}$ (kDa)	$M_{n\,GPC}$ (kDa)	PDI	P_m
1	**1a**	768	95	27.4	38.5	1.32	0.48
2	**1a**	696	92	26.5	44.5	1.40	0.47
3	**1b**	204	92	26.5	24.0	1.82	0.40
4	**1b**	216	96	27.9	27.3	1.49	0.40
5	**A**[b]	40	>99	28.7	22.6	1.09	>0.9
6	**B**[c]	288	85	7.6	7.7	1.06	0.93
7	**D**[d]	0.5	>97	28.5	34.9	1.39	0.74

[a]Entries 1–4: in THF, 80 °C, [catalyst] ≈ 1 mM. Conversions were determined by ^{1}H NMR spectroscopy. M_{ntheo} = molecular weight of chain-end + 144 g mol^{-1} × 200 × conversion. Entries 2–6: in THF (2 mg mL^{-1}). Molecular weights were determined by GPC-LLS (flow rate = 0.5 mL min^{-1}). Universal calibration was carried out with polystyrene standards, using the Mark–Houwink parameters[21] (K = 1.832 × 10^{-4} dL g^{-1}, a = 0.69), laser light scattering detector data, and concentration detector. [b]In toluene, 70 °C, [catalyst]$_o$ ≈ 1 mM, reported by Coates et al.[3a] [c]In toluene, 70 °C, [catalyst]$_o$ ≈ 13 mM, reported by Feijen et al.[4a] [d]In CH_2Cl_2 25 °C, [catalyst] ≈ 1 mM.[14]

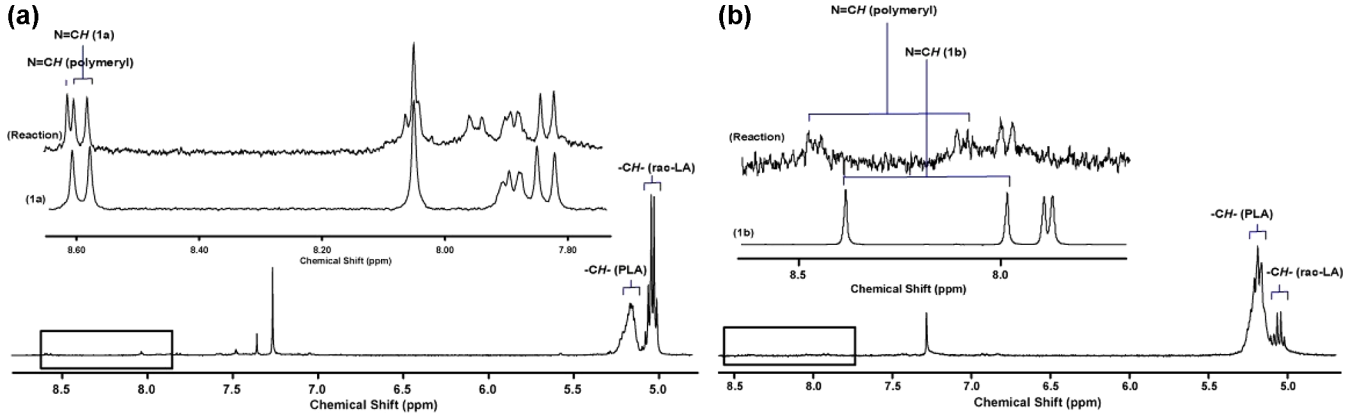

Figure 5. ^{1}H NMR spectra ($CDCl_3$, 25 °C) of (a, left) the reaction of **1a** with 200 equiv of *rac*-LA at ∼50% conversion. Inset shows a ^{1}H NMR spectrum of **1a** overlaid with an expanded region of the spectrum of the reaction and (b, right) the reaction of **1b** with 200 equiv of *rac*-LA at ∼83% conversion. Inset shows a ^{1}H NMR spectrum of **1b** overlaid with an expanded region of the spectrum of the reaction.

Polymerization Studies. Compounds **1a** and **1b** show low activity as catalysts for the ring-opening polymerization of *rac*-LA compared to previously reported dinuclear indium complexes from our group (Table 1).[9c,e,10a,14] Polymerization of 200 equiv of *rac*-LA catalyzed with **1a** (∼1 mM, refluxing THF) reaches 23% conversion after 7 days (>90% conversion was achieved in 30 days.) Complex **1b** reaches 86% conversion in 7 days under identical reaction conditions. Reactions in refluxing toluene occur at a much slower rate with **1a** and **1b**, reaching ∼1% and ∼5% conversion, respectively, after 5 days. In contrast, polymerization of 200 equiv of LA with $[(\kappa^4\text{-ONN}_{Cy}\text{O}_{tBu})\text{In}(\mu\text{-OEt})]_2$ (**D**) reaches >97% conversion in under 30 min at room temperature.[14] The polymer generated by **1b** at full conversion has a heterotactic bias (P_r = 0.61). In contrast, **D** generates largely isotactic PLA (P_m ∼ 0.74). The PLA generated by **1a** is atactic.

The low reactivity of **1a** mimics that of the Al analogue $[(\mu\text{–}\kappa^2\text{-SalBinap})\text{Al}(\mu\text{-OMe})]_2$ (**C**), which is reported to be inactive for lactide polymerization.[8] A comparison of the N=*CH* peaks of **1a** and the resulting polymeryl species after monomer additions shows that even at 50% conversion only ∼30% of **1a** is initiated (Figure 5a). Lack of complete initiation is also supported by the higher-than-expected molecular weights observed (Table 1, entries 1–2). The disparity in the initiation rate may also explain the difference between the calculated and observed M_n values for the polymerizations. Thus, for **1a** the rates of initiation and propagation of polymerization are very slow.

In contrast to complex **1a**, **1b** is a well-controlled catalyst for the polymerization of LA similar to analogous complex $[(\kappa^4\text{-ONN}_{Cy}\text{O}_{tBu})\text{In}(\mu\text{-OEt})]_2$ (**D**). Inspection of a reaction mixture of **1b** and 200 equiv of *rac*-LA at ∼80% conversion shows that the catalyst is fully initiated (Figure 5b). In addition, the theoretical and observed M_n values are in full agreement (Table 1, entries 3–4). GPC analysis of polymerization of 200 equiv of *rac*-LA with **1b** at different conversions shows that the experimental and theoretical M_n values are in close agreement and that PDI values range between 1.2 and 1.8 (Figure 6).

However, polymers obtained with **1b** are very different from those obtained with **D**. Matrix-assisted laser desorption/ionization-time-of-flight (MALDI-TOF) mass spectroscopy of PLA generated with **1b** shows peaks corresponding to the species $[\text{H}(\text{C}_6\text{H}_8\text{O}_4)_n(\text{OC}_2\text{H}_5)\text{Na}]^+$ which are separated by m/z = 144 Da apart (Figure 7). No peaks at m/z = 72 Da intervals are observed, which indicates minimal transesterification in the system under these experimental conditions. In contrast, a MALDI-TOF analysis of polymers generated with **D** show only peaks at m/z = 72 Da indicating extensive transesterification.[14]

A comparison of the results with indium complexes **1b** and **D** shows that their behavior is very different than the analogous aluminum complexes **A** and **B**. Although the SalBinap complex, **A**, is significantly more active than **B**, the qualitative polymerization rates are on the same order (Table 1 entries 5 and 6). In contrast, although complexes **1b** and **D** share the same dimeric structure, complex **D** is a highly active catalyst for LA polymerization, while **1b** is orders of magnitude less reactive. In addition, complexes **A** and **B** show different

dx.doi.org/10.1021/ic500647j | Inorg. Chem. 2014, 53, 6828–6836

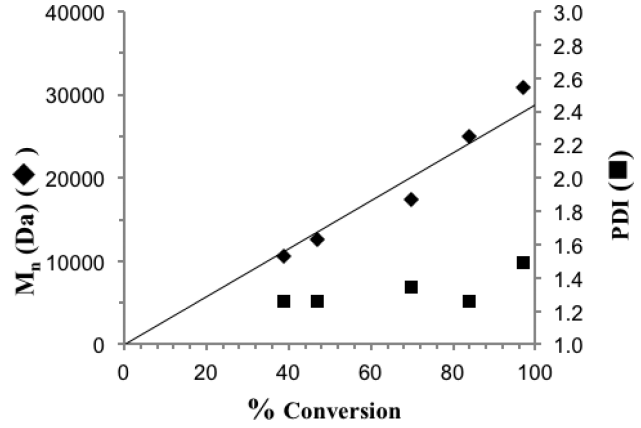

Figure 6. Plot of observed PLA M_n and molecular weight distribution (PDI) vs % conversion for **1b** with LA/initiator ratio of 200/1. The reaction was carried out in refluxing THF, and conversions were obtained using ^{1}H NMR spectroscopy. The line represents the theoretically expected M_n value vs conversion.

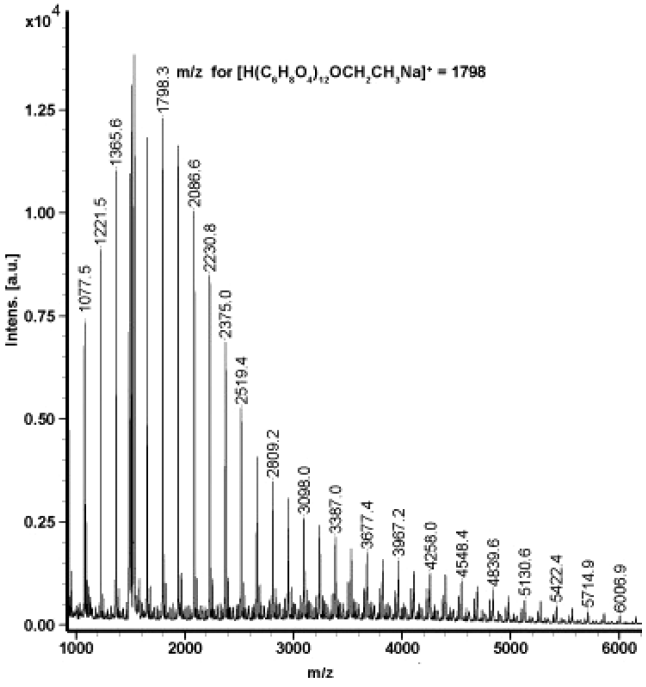

Figure 7. MALDI-TOF mass spectrum of a PLA oligomer grown with **1b**.

transesterification behavior. MALDI-TOF mass spectrometry shows peaks at m/z = 72 Da for polymers obtained with the SalBinap complex **A**,[22] while analogous samples from salen complex, **B**, show no transesterification.[3a,4,8] This pattern is reversed in the case of the indium complexes: SalBinap complex **1b** shows no transesterification, while the salen complex **D** does.[23] Most importantly, the aluminum complexes are isoselective for the polymerization of *rac*-LA ($P_m \sim 0.9$) regardless of the ancillary ligand. In contrast, polymers generated with the two indium complexes show very different microstructures: **1b** is heteroselective, while **D** is isoselective. We do not observe any evidence of a fundamental change in mechanism between the two indium complexes, nor between the aluminum and indium complexes as was observed by Carpentier et al.[6g,12a] Most importantly, the complexes under investigation in our study are indium complexes with monodentate alkoxide ligands which are often dimeric.[9d,10a,14,17] The observed discrepancy is likely due to differences in catalyst structure created by different aggregation behavior in indium alkoxide complexes.

One possible explanation for the low activity of **1b** is that, under polymerization conditions, **1b** converts to inactive **1a**. However, when individual pure samples of **1a** and **1b** are heated in refluxing THF-d_8 or toluene-d_8 for 4 days, complex **1a** remains unchanged and complex **1b** only degrades by <5% (Supporting Information Figures S9 and S10). The low levels of decomposition or conversion of **1b** under the reaction conditions indicates that the effects of these processes on the lowered reaction rates are minimal. Thus, the lower rates observed for **1b** compared to $[(\kappa^4\text{-ONN}_{Cy}\text{O}_{tBu})\text{In}(\mu\text{-OEt})]_2$ (**D**) are likely not caused by a lower initiation rate by the complex.

We investigated the stability of **1b** in the presence of ethyl acetate, a possible LA surrogate, to gain greater information about the mechanism of initiation in the reaction of *rac*-LA with **1b**. A mixture of complex **1b** and 400 equiv of ethyl acetate was stirred at room temperature in THF for 16 h. The ^{1}H NMR spectrum of the mixture, obtained after evaporation of THF and ethyl acetate, shows that **1b** remains unchanged (Supporting Information Figure S14). Under forcing condition, **1b** was stirred for 16 h in neat ethyl acetate at room temperature, after which time the solvent is removed thoroughly. This residue contains a 1:1 mixture of **1b** and a new product (Supporting Information Figure S14). Since the N=C*H* ^{1}H NMR resonances of this product and **1b** are well-resolved it is possible to use the 1:1 mixture to determine the diffusion coefficient of this new species. PGSE spectroscopy of the new product in this mixture gives a diffusion coefficient of 6.2(3) × 10^{-10} m^2 s^{-1}, which is the same as the value for **1b** suggesting that the dimer remains intact. This study indicates that **1b** is a very stable dimer, and the major product from this reaction is also a dimer (Supporting Information Figure S18). We observed similar reactivity with dinuclear indium complexes bearing tridentate ligands.[10a]

■ CONCLUSIONS

We report the synthesis, isolation, and characterization of dinuclear SalBinap indium ethoxide complexes, which are analogous to the benchmark aluminum SalBinap complexes (Chart 1A) introduced by Spassky et al. Through these studies, we are able to compare indium and aluminum complexes bearing salen ligands with either cyclohexyl or binaphthyl (BINAP) backbones. Our studies show that although aluminum complexes with either ligand exhibit similar catalytic activity, as shown by similar reaction rates and selectivity for polymerization of *rac*-LA,[3a,d,4,8] the same is not true for analogous indium complexes.

Aggregation plays an important role in the synthesis of indium(III) complexes. Attempts to synthesize a SalBinap indium alkoxide complex in a one-pot reaction lead to a mixture of two dinuclear compounds **1a** and **1b**, where the ligand is coordinated to the metal centers in κ^2 and κ^4 coordination modes, respectively. The two coordination modes are possible due to the flexibility of the BINAP backbone. Although the κ^2 mode was observed for aluminum complexes (Chart 1B), they could be avoided by using bulky alkoxide initiators.[7] In contrast, our efforts to disrupt the aggregation using either more bulky salen ligands or alkoxide initiators were unsuccessful, supporting the conclusion that the dinuclear nature of these

dx.doi.org/10.1021/ic500647j | Inorg. Chem. 2014, 53, 6828−6836

indium systems is the thermodynamically favored state. Using less bulky unsubstituted ligands also failed to yield tractable products, pointing to the need for a delicate control of sterics to isolate products.

In addition to the difference in synthetic facility, the rates of polymerization for catalysts **1a** and **1b** were orders of magnitude slower than the analogous indium complexes with a cyclohexyl backbone. This result is to be expected for complex **1a** with the κ^2-coordinated ligand, since the analogous aluminum complex is completely unreactive. In contrast, we would have expected complex **1b** to show similar reactivity to the corresponding indium complex with a cyclohexyl backbone $[(\kappa^4\text{-ONN}_{Cy}\text{O}_{tBu})\text{In}(\mu\text{-OEt})]_2$ (Chart 1C). We have ruled out catalyst decomposition or deactivation as the cause, since we observe full activation of the catalyst and obtain experimental polymer molecular weights that match calculated M_n values. Electronic effects are likely not an important factor in these systems; in fact, the aluminum systems with a BINAP backbone are more active than those with a cyclohexyl backbone.[3a,d,4,8]

We speculate that the increased steric bulk in dinuclear complex **1b** is responsible for the sluggish polymerization compared to $[(\kappa^4\text{-ONN}_{Cy}\text{O}_{tBu})\text{In}(\mu\text{-OEt})]_2$. The steric argument is supported by the selectivity observed in the ROP of *rac*-LA by the two catalysts. Complex **1b** is heteroselective while $[(\kappa^4\text{-ONN}_{Cy}\text{O}_{tBu})\text{In}(\mu\text{-OEt})]_2$ is isoselective. This disparity suggests a dominant chain-end control mechanism in **1b**, which can be attributed to the increased sterics of the BINAP backbone compared to the cyclohexyl analogue. This is in marked contrast to what is observed in the analogous aluminum catalysts, which produce highly isotactic PLA regardless of the chiral backbone employed.

Indium complexes with salen and SalBinap ligands behave differently in terms of polymerization activity and selectivity, while nearly identical aluminum analogues behave similarly. This is due to the fact that the indium complexes are dimers and thus have different coordination environments than the mononuclear aluminum complexes with similar coordination environments. Thus, we conclude that, in contrast to aluminum complexes, the larger ionic radius of indium(III) favors aggregation for the alkoxide complexes, is a dominating factor in the chemistry of these species, and must be considered in the development of future stereoselective indium catalysts.

EXPERIMENTAL SECTION

General Considerations. Unless otherwise indicated, all air- and/or water-sensitive reactions were carried out under dry nitrogen using either an MBraun glovebox or standard Schlenk techniques. NMR spectra were recorded on a Bruker Avance 400 or 600 MHz spectrometer. ^{1}H NMR chemical shifts are reported in ppm versus residual protons in deuterated chloroform, δ 7.27 $CDCl_3$. $^{13}C\{^1H\}$ NMR chemical shifts are reported in ppm versus residual ^{13}C in the solvent: δ 77.2 $CDCl_3$. Diffraction measurements for X-ray crystallography were made on a Bruker APEX DUO diffractometer with graphite monochromated Mo Kα radiation. The structures (Supporting Information Table S1) were solved by direct methods and refined by full-matrix least-squares using the SHELXTL crystallographic software of Bruker-AXS. Unless specified, all non-hydrogen atoms were refined with anisotropic displacement parameters, and all hydrogen atoms were constrained to geometrically calculated positions but were not refined. Elemental analysis (C, H, and N) was performed using a Carlo Erba EA1108 elemental analyzer. The elemental composition of unknown samples was determined by using a calibration factor. The calibration factor was determined by analyzing a suitable certified organic standard (OAS) of a known elemental composition. Molecular weights were determined by triple detection gel permeation chromatography (GPC-LLS) using a Waters liquid chromatograph equipped with a Waters 515 HPLC pump, Waters 717 plus autosampler, Phenomenex Phenogel columns (4.6 × 300 mm) 5u 500A, 5u 10E3A and 10E4A, Waters 2410 differential refractometer, Wyatt tristar miniDAWN (laser light scattering detector), and a Wyatt ViscoStar II viscometer. A flow rate of 0.5 mL min^{-1} was used, and samples were dissolved in THF (2 mg mL^{-1}). Narrow molecular weight polystyrene standards were used for calibration purposes. The molar mass was calculated with ASTRA 6 software using the Mark–Houwink parameters K and a from the ViscoStar, laser light scattering detector data, and concentration detector. Mark–Houwink equation gives the relationship between intrinsic viscosity (η) and molar mass (M). Distribution and moment procedures of ASTRA 6 was used to calculate molar mass moments M_n, M_w, and M_z. Atomic absorption spectroscopy was carried out using a PerkinElmer 305A atomic absorption spectrophotometer. Standard solutions of Na for comparison/calibration were prepared using NaCl.

Materials. Solvents (tetrahydrofuran (THF), toluene, hexanes, and diethyl ether) were collected from an MBraun solvent purification system whose columns are packed with activated alumina. THF was further dried over sodium/benzophenone, distilled under vacuum, and degassed. EtOAc, CH_2Cl_2, and acetonitrile were dried over CaH_2, distilled under vacuum, and degassed. $CDCl_3$ was dried over CaH_2, and degassed through a series of freeze–pump–thaw cycles. Toluene-d_8 and THF-d_8 from Cambridge Isotope Laboratories, Inc., were dried over sodium/benzophenone, distilled under vacuum, and degassed through a series of freeze–pump–thaw cycles. *rac*-LA was a gift from PURAC America Inc. and recrystallized thrice from hot dry toluene. *rac*-1,1′-Binaphthyl-2,2′-diamine, potassium *tert*-butoxide, and sodium ethoxide (washed with ethanol and hexanes prior to use) were purchased from Alfa Aesar. $InCl_3$ was purchased from Strem Chemicals Inc. *rac*-2,2′-[1,1′-Binaphthalene-2,2′-diyl-bis-(nitrilomethylidyne)]-bis(*E*,*E*)-4,6-di-*tert*-butylphenol and 4-*tert*-butyl-6-methylsalicylaldehyde were prepared according to literature procedures.[20,24]

Synthesis of (±)-H$_2$(ONN*O$_{Me}$). A 50 mL round bottomed flask was charged with a racemic mixture of 1,1′-binaphthyl-2,2-diamine (0.222 g, 0.780 mmol), 2 equiv of 4-*tert*-butyl-6-methylsalicylaldehyde (0.300 mg, 1.56 mmol), 25 mL of ethanol, and a magnetic stir bar. A catalytic amount of formic acid (1 drop) was then introduced to the stirring yellow mixture which was subsequently heated to reflux at 80 °C for 3 h. Heating was discontinued, and the bright yellow precipitate was suction filtered and washed once with cold ethanol (5 mL). The product was subsequently dried under reduced pressure and used without further purification (462 mg, 94%). ^{1}H NMR (600 MHz, $CDCl_3$): 12.00 (bs, 1H, Ar–O*H*), 8.60 (s, 1H, Ar–C*H*N–), 8.04 (d, J = 8.8 Hz, 1H, Ar–*H*), 7.94 (d, J = 8.2 Hz, 1H, Ar–*H*), 7.55 (d, J = 8.8 Hz, 1H, Ar–*H*), 7.42 (dd, J = 10.8, 3.9 Hz, 1H, Ar–*H*), 7.22 (d, J = 8.3 Hz, 1H, Ar–*H*), 7.11 (s, 1H, Ar–*H*), 7.03 (d, J = 2.1 Hz, 1H, Ar–*H*), 2.05 (s, 3H, Ar–C*H*$_3$), 1.23 (s, 9H, Ar–(C*H*$_3$)$_3$). $^{13}C\{H\}$ NMR (151 MHz, $CDCl_3$): 163.28, 157.17, 144.81, 140.75, 133.49, 132.51, 131.61, 129.91, 128.91, 128.34, 126.97, 126.59, 126.28, 125.68, 125.54, 118.01, 117.99, 33.96, 31.55, 15.84. Anal. Calcd for $C_{44}H_{44}N_2O_2$: C, 83.51; H, 7.01; N, 4.43. Found: C, 83.17; H, 7.01; N, 4.48.

Synthesis of 1a and 1b. A solution of (±)-H$_2$(**ONN*O$_{Me}$**) in 10 mL of toluene (144 mg, 0.23 mmol) was added to 8 equiv of NaOEt (121 mg, 1.82 mmol) in a 20 mL scintillation vial. A magnetic stir bar was added, and the reaction proceeded for 30 min at room temperature before addition of 1.3 equiv of anhydrous $InCl_3$ (71 mg, 0.29 mmol). After overnight stirring, the solution was filtered and evaporated under vacuum. The yellow solid was resuspended in 20 mL of acetonitrile, filtered, and washed with 1 mL of acetonitrile. The resuspension and filtration of the solid precipitate was repeated two more times. The filtrate and wash contained **1a** (60 mg, 32%) while the undissolved solid was **1b** (35.6 mg, 19%). Data for **1a** follow. ^{1}H NMR (400 MHz, $CDCl_3$): δ 8.61 (s, 1H, N=C*H*), 8.58 (s, 1H, N=C*H*), 8.05 (s, 2H, Ar–*H*), 7.90–7.81 (m, 4H, Ar–*H*), 7.52–7.49 (m, 6H Ar–*H*), 7.06–7.05 (d, 2H, Ar–*H*), 2.85–2.75 (m, 1H, –OC*H*$_A$H$_B$–), 2.37 (s, 6H, Ar–C*H*$_3$), 2.16–2.05 (m, 1H, –OCH$_A$*H*$_B$–), 1.00 (s, 18H, Ar–C(CH$_3$)$_3$), −0.44 (t, 3H,

dx.doi.org/10.1021/ic500647j | Inorg. Chem. 2014, 53, 6828–6836

$-OCH_2-CH_3$). ^{13}C NMR (151 MHz, $CDCl_3$): δ 174.11, 167.45, 149.17, 135.88, 134.69, 133.42, 131.62, 129.06, 128.20, 127.93, 127.07, 126.93, 126.35, 125.31, 124.63, 116.11, 60.97, 32.94, 30.88, 29.49, 18.23. Anal. Calcd for $C_{92}H_{94}In_2N_4O_6$: C, 69.87; H, 5.99; N, 3.54. Found: C, 72.16; H, 6.28; N, 3.67. Data for **1b** follow. ^1H NMR (400 MHz, $CDCl_3$): 8.33 (s, 1H, N=C*H*), 7.93 (s, 1H, N=C*H*), 7.84 (s, 1H, Ar−*H*), 7.82 (s, 1H, Ar−*H*), 7.56−7.53 (d, 1H, Ar−*H*), 7.40−7.13 (m, 8H, Ar−*H*), 7.07−7.04 (d, 1H, Ar−*H*), 6.75 (d, 1H, Ar−*H*), 6.68 (d, 1H, Ar−*H*), 6.46−6.43 (d, J = 12 Hz, 1H, Ar−*H*), 2.45−2.37 (m, 1H, $-OCH_AH_B-$), 2.01 (s, 3H, Ar−CH_3), 1.96−1.92 (m, 1H, $-OCH_AH_B-$), 1.87 (s, 3H, Ar−CH_3), 1.35 (s, 9H, Ar−$C(CH_3)_3$), 1.23 (s, 9H, Ar−$C(CH_3)_3$), 0.50 (t, 3H, $-OCH_2CH_3$). ^{13}C NMR (151 MHz, $CDCl_3$): δ 173.51, 172.01, 169.20, 168.64, 147.63, 146.16, 137.04, 135.82, 133.90, 133.84, 132.95, 132.68, 132.64, 132.10, 131.87, 131.72, 129.95, 129.09, 128.28, 128.15, 128.01, 127.50, 127.07, 126.67, 126.60, 126.37, 126.29, 126.04, 125.18, 124.49, 123.71, 118.16, 116.68, 59.75, 33.66, 33.56, 31.48, 31.223, 19.90, 18.68, 16.64. Anal. Calcd for $C_{92}H_{94}In_2N_4O_6$: C, 69.87; H, 5.99; N, 3.54. Found: C, 69.27; H, 5.86; N, 3.52. Na content for both complexes by atomic absorption spectroscopy <0.005% wt.

Synthesis of 2. A 20 mL scintillation vial was charged with a Teflon stir bar, potassium *tert*-butoxide (0.651 g, 5.80 mmol), and 2 mL of THF. The mixture was allowed to stir until complete dissolution of KO^tBu was achieved. The ligand (±)-H_2(**ONN*O$_{Me}$**) (0.210 g, 2.93 mmol) was dissolved in 2 mL of THF and added to the stirring solution. The mixture was stirred for 3 h. At this point a suspension of anhydrous $InCl_3$ (0.650 g, 2.94 mmol) in THF (2 mL) was added to reaction and stirred for another 6 h. The mixture was then filtered through glass filter paper, and the volatile components were evaporated under vacuum to afford a yellow solid. This was redissolved in diethyl ether and allowed to crystallize at −35 °C. The final product was obtained as a yellow crystalline solid (1.50 g, 59%) which was filtered and dried under vacuum. ^1H NMR (400 MHz, CDCl3): 8.48 (s(br), 2H, N=C*H*), 8.06−8.05 (d, 2H, Ar−*H*), 7.95−7.94 (d, 2H, Ar−*H*), 7.50−7.42 (m, 6H, Ar−*H*), 7.26−7.24 (m, 2H, Ar−*H*), 6.91 (s(br), 4H, Ar−*H*), 1.47 (s, 18H, Ar−$C(CH_3)_3$), 1.24 (s, 18H, Ar−$C(CH_3)_3$). ^{13}C NMR (151 MHz, $CDCl_3$): δ 142.89, 138.04, 133.46, 132.38, 130.62, 129.55 127.17, 126.55, 126.07, 124.51, 36.61, 33.98, 31.12, 29.48. Anal. Calcd for $C_{50}H_{54}InClN_2O_2$: C, 69.41; H, 6.29; N, 3.24. Found: C, 70.31; H, 6.40; N, 3.07.

Polymerization of Lactide (Representative Procedure). In a 20 mL scintillation vial (inside the glovebox, nitrogen atmosphere), **1b** (4 mg, 0.0025 mmol) was dissolved in 1 mL of THF, and *rac*-lactide (0.146 g, 1.01 mmol) in 1.5 mL of THF was added. The solution was transferred to Teflon screw-capped dry Schlenk flask. The reaction was removed from the glovebox and allowed to stir under reflux in an oil bath at 80 °C for 9 days. The flask was taken back inside the box, and a 0.5 mL sample of the reaction mixture was evaporated under vacuum for 3 h and was dissolved in $CDCl_3$. $^1H\{^1H\}$ NMR spectrum of the methine region was obtained on a Bruker 600 MHz spectrometer. Thereafter, the mixture was transferred out of the glovebox into a 20 mL vial and quenched with two drops of 1 M HCl in diethyl ether. The solvent was evaporated under vacuum, and the polymer was isolated by washing 3 times with cold methanol. The isolated polymer was subsequently dried under vacuum for 4 h prior to GPC analysis. For the experiments where GPC data was obtained at partial conversions, the reaction mixture was taken back into the glovebox, and a sample was withdrawn for analysis.

Monitoring the Thermal Stability of Catalysts (Representative Procedure). A Teflon sealed NMR tube was charged with a solution of **1b** (5 mg (0.0031 mmol) dissolved in 0.5 mL of THF-d_8), and a ^1H NMR spectrum was obtained. The tube was allowed to sit in an oil bath at 80 °C, and ^1H NMR spectra were obtained every 24 h for 4 days.

Conversion of 1b to 1a with NaOEt. A 20 mL scintillation vial was charged with 61 mg (0.038 mmol) of **1b** and 13 mg (0.19 mmol) of NaOEt and stirred for 16 h in 1 mL of toluene. The solvent was evaporated under vacuum, and a ^1H NMR spectrum was obtained of the yellow solid residue.

Reaction of 1b with Ethyl Acetate. A 20 mL scintillation vial was charged with 5 mg (0.0031 mmol) of **1b** dissolved in 1 mL of THF, and 125 μL (0.63 mmol) of dry EtOAc was added and stirred for 16 h at ambient temperature. The solvent was evaporated under vacuum, and a ^1H NMR spectrum was obtained of the yellow solid residue. The procedure was similar for the experiment with neat ethyl acetate. However, no THF was used, and the complex was simply dissolved in 1 mL of ethyl acetate. For PGSE NMR studies a portion of the dry reaction mixture (after a 16 h reaction in neat ethyl acetate and evaporation of volatile components under vacuum; 3.5 mg, [In] ~ 4 mM) was dissolved in a 1 mL volumetric flask with a solution of tetrakis(trimethylsilyl)silane (TMSS) (0.94 mM) in CD_2Cl_2. The N=C*H* ^1H NMR resonance at 8.41 ppm was used for the analysis.

Representative Sample Preparation with (ONN*O)H_2 for PGSE NMR Studies. In a 1 mL volumetric flask, 2.8 mg of (ONN*O)H_2 (0.0044 mmol, 0.0044 M) was made with a solution of tetrakis(trimethylsilyl)silane (TMSS) (0.94 mM in CD_2Cl_2) also used as an internal standard. A 0.5 mL volume was transferred into a Teflon capped sealed NMR tube for spectroscopy.

MALDI-TOF Mass Spectroscopy on PLA Oligomers. In a 20 mL scintillation vial (inside the glovebox, nitrogen atmosphere) **1b** (3 mg, 0.0019 mmol) was dissolved in 0.5 mL of THF, and *rac*-lactide (0.014 g, 0.097 mmol) in 0.5 mL of THF was added. The solution was transferred to Teflon screw-capped dry Schlenk flask. The reaction was removed from the glovebox and allowed to stir under reflux in an oil bath at 80 °C for 16 h. Thereafter the mixture was transferred out of the glovebox into a 20 mL vial and quenched with two drops of 1 M HCl in diethyl ether. The solvent was evaporated under vacuum, and the polymer was isolated by washing 3 times with cold methanol. The isolated polymer was subsequently dried under vacuum for 4 h prior to analysis. Matrix-assisted laser desorption/ionization time-of-flight (MALDI-TOF) mass spectrometric analysis was performed on a Bruker Autoflex MALDI-TOF equipped with a nitrogen laser (337 nm). The accelerating potential of the Bruker instrument was 19.5 kV. The polymer samples were dissolved in THF (ca. 1 g/mL). The concentration of a cationization agent, sodium trifluoroacetate, in THF was 1 mM. The matrix used was *trans*-2-[3-(4-*tert*-butylphenyl)2-methyl-2-propenylidene]malononitrile (DCTB) at a concentration of 20 mg/mL. A sample solution was prepared by mixing polymer, matrix, and salt in a volume ratio of 5:5:1, respectively. The mixed solution was spotted on a stainless steel target and then left to dry at room temperature. The spectra were collected in a linear mode.

■ ASSOCIATED CONTENT

Ⓢ Supporting Information

Structure and solution phase characterization of compounds. Crystallographic data in CIF format. This material is available free of charge via the Internet at http://pubs.acs.org.

■ AUTHOR INFORMATION

Corresponding Author

*E-mail: mehr@chem.ubc.ca.

Notes

The authors declare no competing financial interest.

■ ACKNOWLEDGMENTS

D.C.A. thanks Dr. Brian O. Patrick for helpful discussions regarding refining X-ray structures. E.X.Y. thanks NSERC and the Inorganic Chemistry Exchange program for a summer undergraduate research award. The authors would like to acknowledge NSERC for funding this work.

■ REFERENCES

(1) (a) Dijkstra, P. J.; Du, H. Z.; Feijen, J. *Polym. Chem.* **2011**, *2* (3), 520−527. (b) Thomas, C. M. *Chem. Soc. Rev.* **2010**, *39* (1), 165−173. (c) Stanford, M. J.; Dove, A. P. *Chem. Soc. Rev.* **2010**, *39* (2), 486−494. (d) Kamber, N. E.; Jeong, W.; Waymouth, R. M.; Pratt, R. C.;

Lohmeijer, B. G. G.; Hedrick, J. L. *Chem. Rev.* **2007**, *107* (12), 5813−5840. (e) Fukushima, K.; Kimura, Y. *Polym. Int.* **2006**, *55* (6), 626−642. (f) Dechy-Cabaret, O.; Martin-Vaca, B.; Bourissou, D. *Chem. Rev.* **2004**, *104* (12), 6147−6176.
(2) Spassky, N.; Wisniewski, M.; Pluta, C.; LeBorgne, A. *Macromol. Chem. Phys.* **1996**, *197* (9), 2627−2637.
(3) (a) Ovitt, T. M.; Coates, G. W. *J. Polym. Sci., Part A: Polym. Chem.* **2000**, *38*, 4686−4692. (b) Radano, C. P.; Baker, G. L.; Smith, M. R. *J. Am. Chem. Soc.* **2000**, *122* (7), 1552−1553. (c) Chisholm, M. H.; Patmore, N. J.; Zhou, Z. P. *Chem. Commun.* **2005**, *1*, 127−129. (d) Ovitt, T. M.; Coates, G. W. *J. Am. Chem. Soc.* **1999**, *121* (16), 4072−4073.
(4) (a) Zhong, Z. Y.; Dijkstra, P. J.; Feijen, J. *Angew. Chem., Int. Ed.* **2002**, *41* (23), 4510−4513. (b) Zhong, Z. Y.; Dijkstra, P. J.; Feijen, J. *J. Am. Chem. Soc.* **2003**, *125* (37), 11291−11298.
(5) (a) Nomura, N.; Ishii, R.; Akakura, M.; Aoi, K. *J. Am. Chem. Soc.* **2002**, *124* (21), 5938−5939. (b) Hormnirun, P.; Marshall, E. L.; Gibson, V. C.; White, A. J. P.; Williams, D. J. *J. Am. Chem. Soc.* **2004**, *126* (9), 2688−2689. (c) Ishii, R.; Nomura, N.; Kondo, T. *Polym. J.* **2004**, *36* (3), 261−264. (d) Tang, Z. H.; Chen, X. S.; Pang, X.; Yang, Y. K.; Zhang, X. F.; Jing, X. B. *Biomacromolecules* **2004**, *5* (3), 965−970. (e) Tang, Z. H.; Chen, X. S.; Yang, Y. K.; Pang, X.; Sun, J. R.; Zhang, X. F.; Jing, X. B. *J. Polym. Sci., Part A: Polym. Chem.* **2004**, *42* (23), 5974−5982. (f) Hormnirun, P.; Marshall, E. L.; Gibson, V. C.; Pugh, R. I.; White, A. J. P. *Proc. Natl. Acad. Sci. U.S.A.* **2006**, *103* (42), 15343−15348. (g) Nomura, N.; Ishii, R.; Yamamoto, Y.; Kondo, T. *Chem.—Eur. J.* **2007**, *13* (16), 4433−4451. (h) Bouyahyi, M.; Grunova, E.; Marquet, N.; Kirillov, E.; Thomas, C. M.; Roisnel, T.; Carpentier, J. F. *Organometallics* **2008**, *27* (22), 5815−5825. (i) Alaaeddine, A.; Thomas, C. M.; Roisnel, T.; Carpentier, J. F. *Organometallics* **2009**, *28* (5), 1469−1475. (j) Bouyahyi, M.; Roisnel, T.; Carpentier, J. F. *Organometallics* **2010**, *29* (2), 491−500. (k) Nomura, N.; Akita, A.; Ishii, R.; Mizuno, M. *J. Am. Chem. Soc.* **2010**, *132* (6), 1750−1751.
(6) (a) Bakewell, C.; Cao, T. P. A.; Long, N.; Le Goff, X. F.; Auffrant, A.; Williams, C. K. *J. Am. Chem. Soc.* **2012**, *134* (51), 20577−20580. (b) Kapelski, A.; Okuda, J. *J. Polym. Sci., Part A: Polym. Chem.* **2013**, *51* (23), 4983−4991. (c) Hancock, S. L.; Mahon, M. F.; Jones, M. D. *Dalton Trans.* **2013**, *42* (25), 9279−9285. (d) Gao, B.; Duan, R. L.; Pang, X.; Li, X.; Qu, Z.; Tang, Z. H.; Zhuang, X. L.; Chen, X. S. *Organometallics* **2013**, *32* (19), 5435−5444. (e) Cross, E. D.; Allan, L. E. N.; Decken, A.; Shaver, M. P. *J. Polym. Sci., Part A: Polym. Chem.* **2013**, *51* (5), 1137−1146. (f) Bakewell, C.; White, A. J. P.; Long, N. J.; Williams, C. K. *Inorg. Chem.* **2013**, *52* (21), 12561−12567. (g) Normand, M.; Kirillov, E.; Roisnel, T.; Carpentier, J. F. *Organometallics* **2012**, *31* (4), 1448−1457. (h) Matsubara, K.; Terata, C.; Sekine, H.; Yamatani, K.; Harada, T.; Eda, K.; Dan, M.; Koga, Y.; Yasuniwa, M. *J. Polym. Sci., Part A: Polym. Chem.* **2012**, *50* (5), 957−966. (i) Horeglad, P.; Szczepaniak, G.; Dranka, M.; Zachara, J. *Chem. Commun.* **2012**, *48* (8), 1171−1173. (j) Chen, H. L.; Dutta, S.; Huang, P. Y.; Lin, C. C. *Organometallics* **2012**, *31* (5), 2016−2025. (k) Ma, W. A.; Wang, Z. X. *Organometallics* **2011**, *30* (16), 4364−4373. (l) Schwarz, A. D.; Chu, Z. Y.; Mountford, P. *Organometallics* **2010**, *29* (5), 1246−1260. (m) Qian, F.; Liu, K. Y.; Ma, H. Y. *Dalton Trans.* **2010**, *39* (34), 8071−8083. (n) Horeglad, P.; Kruk, P.; Pecaut, J. *Organometallics* **2010**, *29* (17), 3729−3734. (o) Kushwah, N. P.; Pal, M. K.; Wadawale, A. P.; Jain, V. K. *J. Organomet. Chem.* **2009**, *694* (15), 2375−2379. (p) Du, H. Z.; Velders, A. H.; Dijkstra, P. J.; Sun, J. R.; Zhong, Z. Y.; Chen, X. S.; Feijen, J. *Chem.—Eur. J.* **2009**, *15* (38), 9836−9845. (q) Broderick, E. M.; Diaconescu, P. L. *Inorg. Chem.* **2009**, *48* (11), 4701−4706. (r) Aiello, I.; Aiello, D.; Ghedini, M. *J. Coord. Chem.* **2009**, *62* (20), 3351−3365. (s) Zhang, C.; Wang, Z. X. *J. Organomet. Chem.* **2008**, *693* (19), 3151−3158. (t) Jin, G. X.; Jones, C.; Junk, P. C.; Stasch, A.; Woodul, W. D. *New J. Chem.* **2008**, *32* (5), 835−842. (u) Chisholm, M. H.; Gallucci, J. C.; Quisenberry, K. T.; Zhou, Z. P. *Inorg. Chem.* **2008**, *47* (7), 2613−2624. (v) Tang, Z. H.; Gibson, V. C. *Eur. Polym. J.* **2007**, *43* (1), 150−155. (w) Lian, B.; Thomas, C. M.; Casagrande, O. L.; Lehmann, C. W.; Roisnel, T.; Carpentier, J. F. *Inorg. Chem.* **2007**, *46* (1), 328−340. (x) Du, H. Z.; Pang, X.; Yu, H. Y.; Zhuang, X. L.; Chen, X. S.; Cui, D. M.; Wang, X. H.; Jing, X. B. *Macromolecules* **2007**, *40* (6), 1904−1913. (y) Wu, J. C.; Yu, T. L.; Chen, C. T.; Lin, C. C. *Coord. Chem. Rev.* **2006**, *250* (5−6), 602−626.
(7) Atwood, D. A.; Jegier, J. A.; Rutherford, D. *Inorg. Chem.* **1996**, *35* (1), 63−70.
(8) Ovitt, T. M.; Coates, G. W. *J. Am. Chem. Soc.* **2002**, *124* (7), 1316−1326.
(9) (a) Aluthge, D. C.; Xu, C. L.; Othman, N.; Noroozi, N.; Hatzikiriakos, S. G.; Mehrkhodavandi, P. *Macromolecules* **2013**, *46* (10), 3965−3974. (b) Xu, C.; Yu, I.; Mehrkhodavandi, P. *Chem. Commun.* **2012**, *48* (54), 6806−6808. (c) Osten, K. M.; Yu, I.; Duffy, I. R.; Lagaditis, P. O.; Yu, J. C. C.; Wallis, C. J.; Mehrkhodavandi, P. *Dalton Trans.* **2012**, *41* (26), 8123−8134. (d) Acosta-Ramirez, A.; Douglas, A. F.; Yu, I.; Patrick, B. O.; Diaconescu, P. L.; Mehrkhodavandi, P. *Inorg. Chem.* **2010**, *49* (12), 5444−5452. (e) Douglas, A. F.; Patrick, B. O.; Mehrkhodavandi, P. *Angew. Chem., Int. Ed.* **2008**, *47* (12), 2290−2293.
(10) (a) Yu, I.; Acosta-Ramirez, A.; Mehrkhodavandi, P. *J. Am. Chem. Soc.* **2012**, *134* (30), 12758−12773. (b) Fang, J.; Yu, I.; Mehrkhodavandi, P.; Maron, L. *Organometallics* **2013**, *32*, 6950−6956.
(11) Dagorne, S.; Normand, M.; Kirillov, E.; Carpentier, J. F. *Coord. Chem. Rev.* **2013**, *257* (11−12), 1869−1886.
(12) (a) Normand, M.; Dorcet, V.; Kirillov, E.; Carpentier, J. F. *Organometallics* **2013**, *32* (6), 1694−1709. (b) Maudoux, N.; Roisnel, T.; Dorcet, V.; Carpentier, J. F.; Sarazin, Y. *Chem. Eur. J.* **2014**, *20*, DOI: 10.1002/chem.201304788.
(13) (a) Atwood, D. A.; Jegier, J. A.; Rutherford, D. *Bull. Chem. Soc. Jpn.* **1997**, *70* (9), 2093−2100. (b) Hill, M. S.; Atwood, D. A. *Main Group Chem.* **1998**, *2* (3), 191−202. (c) Atwood, D. A.; Harvey, M. J. *Chem. Rev.* **2001**, *101* (1), 37−52.
(14) Aluthge, D. C.; Patrick, B. O.; Mehrkhodavandi, P. *Chem. Commun.* **2013**, *49* (39), 4295−4297.
(15) Abraham, R. J.; Canton, M.; Reid, M.; Griffiths, L. *J. Chem. Soc., Perkin Trans. 2* **2000**, *4*, 803−812.
(16) Ionic radii for six-coordinate: Al^{3+}, 0.535 Å; In^{3+}, 0.80 Å: Shannon, R. D. *Acta Crystallogr., Sect. A* **1976**, *A32*, 751.
(17) Peckermann, I.; Kapelski, A.; Spaniol, T. P.; Okuda, J. *Inorg. Chem.* **2009**, *48* (12), 5526−5534.
(18) Macchioni, A.; Ciancaleoni, G.; Zuccaccia, C.; Zuccaccia, D. *Chem. Soc. Rev.* **2008**, *37* (3), 479−489.
(19) Silvernail, C. M.; Yao, L. J.; Hill, L. M. R.; Hillmyer, M. A.; Tolman, W. B. *Inorg. Chem.* **2007**, *46* (16), 6565−6574.
(20) Bernardo, K. D. S.; Robert, A.; Dahan, F.; Meunier, B. *New J. Chem.* **1995**, *19* (2), 129−131.
(21) Podzimek, S. Light Scattering, Size Exclusion Chromatography and Asymmetric Flow Field Flow Fractionation: Powerful Tools for the Characterization of Polymers. *Proteins and Nanoparticles*; John Wiley & Sons: Hoboken, NJ, 2011; pp 23−34.
(22) Montaudo, G.; Montaudo, M. S.; Puglisi, C.; Samperi, F.; Spassky, N.; LeBorgne, A.; Wisniewski, M. *Macromolecules* **1996**, *29* (20), 6461−6465.
(23) Aluthge, D. C.; Mehrkhodavandi, P. In preparation.
(24) Rudzevich, V.; Schollmeyer, D.; Braekers, D.; Desreux, J. F.; Diss, R.; Wipff, G.; Bohmer, V. *J. Org. Chem.* **2005**, *70* (15), 6027−6033.